Nat. Hazards Earth Syst. Sci. Discuss., https://doi.org/10.5194/nhess-2019-90
Manuscript under review for journal Nat. Hazards Earth Syst. Sci.
Discussion started: 23 April 2019

Natural Hazards and Earth System Sciences
Open Access
Discussions

# Landslides distribution at tributaries with different evolution stages in Jiangjia Gully, southwestern China

Xia Fei Tian [a, b, c], Yong Li [a, b*], Quan Yan Tian [c, d], Feng Huan Su [a, b]

a. Key Laboratory of Mountain Hazards and Surface Process, CAS, Chengdu, 610041, China
b. Institute of Mountain Hazards and Environment, CAS, Chengdu, 610041, China
c. University of Chinese Academy of Sciences, Beijing 100049, China
d. Cold and Arid Region of Environmental and Engineering Research Institute, CAS

*Corresponding author: Li Yong
E-mail: ylie@imde.ac.cn

**Abstract:** Jiangjia Gully (JJG) is known for its high frequency and variety of debris flows, especially the intermittent surges of various flow regimes and materials. Observation indicates that the surges come from various tributaries with different landslides activities. In this study, 81 tributaries of JJG are taken from DEM with 10 m grid cells, and the hypsometric curves are used to characterize their evolution stages; five stages are identified by the evolution index (EI, the integral of the hypsometric curves) and most tributaries are in relative youth stage with EI between 0.5 and 0.6. Then 908 landslides are interpreted from Quickbird satellite image of 0.61 m resolution, and it is found that LD (LD = landslides number in a tributary/ the tributary area) increases exponentially with EI, while $LA_p$ ( $LA_p$ = landslides area in a tributary/ the tributary area) fluctuates with EI, meaning that landslides are inclined to occur in tributaries with EI between 0.5 and 0.6, and thus these tributaries are the main material sources supplying for debris flows.

**Key words:** Hypsometric curve; Evolution stages; Tributaries; Landslides distribution

## 1 Introduction

Geomorphic evolution has been one of the important research topics in geomorphology, hypsometric analysis has been used to deal with erosional topography and the process of landform development (Bartolini et al., 2003; Li et al., 2011; Lv et al., 2005). Strahler (1952) asserted that different types of landform have different characteristic shape of their hypsometric curves, dividing landform into 'young' and 'mature' with the hypsometric integral decreasing. In this meaning, the integral can be defined as the evolution index (EI) of the tributary. Meanwhile, the hypsometric curves are related to tributary form and erosional process, and are used to interpret landform development stages (Schumm, 1956; Strahler, 1952, 1957). In addition, the relationship between EI and tributary characteristics changes with scales. For example, the dissection index of tributaries presents various relationships to EI depending on scale of the tributaries. For the 5th-order tributaries, their correlation is r = 0.41, whereas for the 4th-order, it is r = 0.24, and it becomes negative correlation for the 3rd-order (Hamza V et al., 2018). Combined with the results of field investigation, this study adopts the tributary scale that debris flow easily occurs to meet our research needs.

For a given watershed, especially a small gully in mountains (below 100 $km^2$ and most below 10 $km^2$), the tributaries with different EI present various topographic characteristics. Similarly, significant difference exists in the distribution of landslides among various tributaries, landslides are frequent in some tributaries while occasional in others (Baum et al., 2005; Pradhan and Sameen, 2017; Wang et al., 2006; Wieczorek, 1996). Although landslides distribution per se are influenced by many factors, such as lithology, topographic characteristics (Langebein and Basil, 2007) and climatic variable (Huggel et al., 2005; Wieczorek and Glade, 2005), and the specific evolution state of a tributary is the result affected by these comprehensive factors as well. Therefore, the relationship between EI and landslides distribution has special significance to reveal the landslides distribution characteristics with regards to mountainous tributaries, which, however, has gotten little attentions in literatures.

In this paper, a case study is conducted in Jiangjia Gully (JJG), where weak and similar lithology, disparate topography, sparse vegetation, and unconsolidated deposits are widely distributed in tributaries. In addition, it is known for the high variety of debris flows; each debris-flow event consists of tens or hundreds surges of different flow regimes, velocities, discharges, and total volumes (Li et al., 2015; Li et al., 2013; Arai, 2017). In particular, the surges are composed of different materials, suggesting that they come from different sources (Xiang et al., 2015). In other words, each debris flow in JJG comes from different tributaries (Bollschweiler et al., 2007; Li et al., 2012; Li et al., 2013; Li et al., 2015). Moreover, the debris flow behaviors in JJG are representative and similar phenomena are subsistent in other parts of the world. Generally, the flow surges are originated from different tributaries and the material supplies are mainly from landslides (including avalanches, soil failures and other slope processes) (Beguería, 2006). So the study of landslides distribution in different evolution stages is of great significance to reveal the landslides distribution characteristics of the tributaries with similar lithology and disparate topography, but also can roughly determine the material supply and explain the formation mechanism of debris flow surges.

## 2 Study area and data collection

### 2.1 Setting of the study area

JJG is located in the Xiaojiang River of the Upper Changjiang River. The mainstream channel length is $1.39\times10^4$ m and the gully area is $4.84\times10^7$ $m^2$ (Fig. 1). This region undergoes active neotectonic movement, faults, and folds; and rocks are dominated by slate, dolomite, limestone, basalt and breccia rocks, which are easily weathered (Gabet and Mudd, 2006). Generally, weak lithology, wide faults and sparse vegetation are the obvious characteristics of the gully, and the tributaries are in steep topography and intense landslide activity, with wide distribution of quaternary unconsolidated deposits. Loose materials are widely distributed in the gully and debris flows occur frequently, which are the major material sources for the debris flows. According to the statistics data, the landslides area reaches 16.4 $km^2$ that accounts for 39.7% of the gully area. As well, average annual sediment yield by debris flow is about $1.54\times10^6$ $m^3$ (Wu et al., 1990; Zhuang et al., 2015).

Nat. Hazards Earth Syst. Sci. Discuss., https://doi.org/10.5194/nhess-2019-90
Manuscript under review for journal Nat. Hazards Earth Syst. Sci.
Discussion started: 23 April 2019



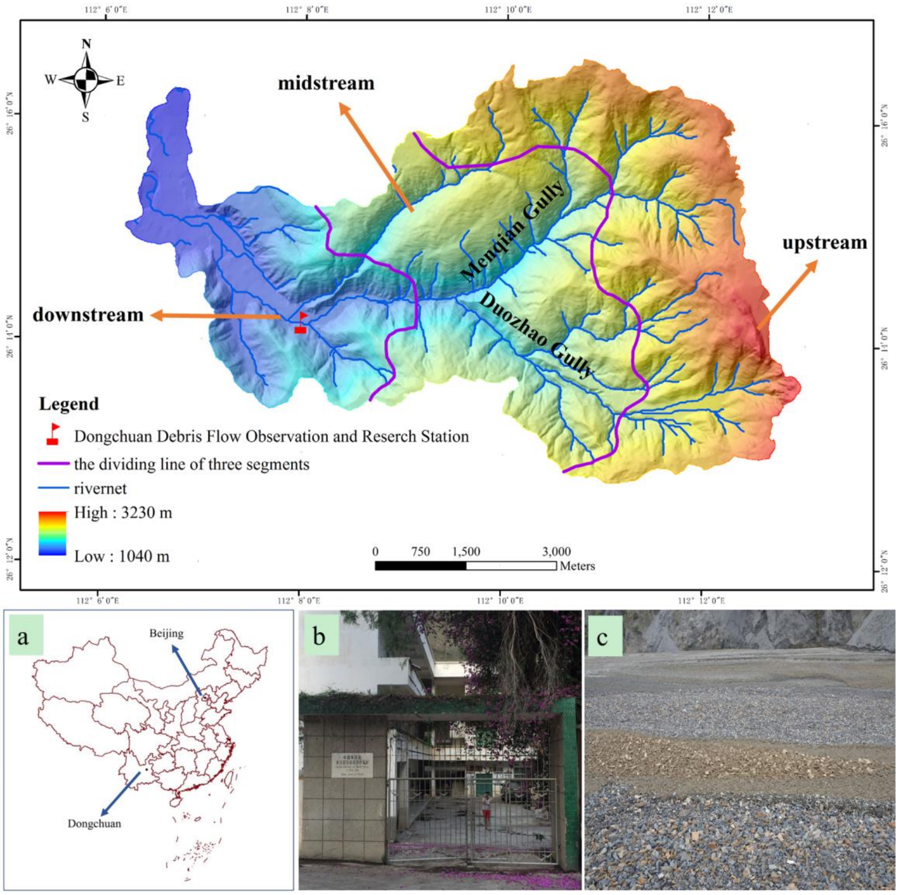


**Fig. 1** The location of JJG. a The location of Dongchuan in China. b Dongchuan Debris Flow Observation and research stations. c Deposition of surges.

The most remarkable features of debris flow in JJG are the high frequency in occurrence and great variety of flow regime and magnitude. Each occurrence contains tens to hundreds of surges (Li et al., 2012); the surges are separated in time and space, and different from one another in density, velocity, and sediment concentration. The variation of flow velocity with density is shown in Fig. 2, which contains surges in one single event on July 12, 2017.

The great variety of surges densities, with different material compositions, can be attributed to different sources; this means that even a single surge material comes from different tributaries in most cases (Webb et al., 1989). As observed in the last decades, debris flows almost come from the north branch, the Menqian Gully, while the south branch, the Duozhao Gully, is often silent. This presents the gross distinction of material and landslides activities in JJG, which further implies that there must be more differences in tributaries.

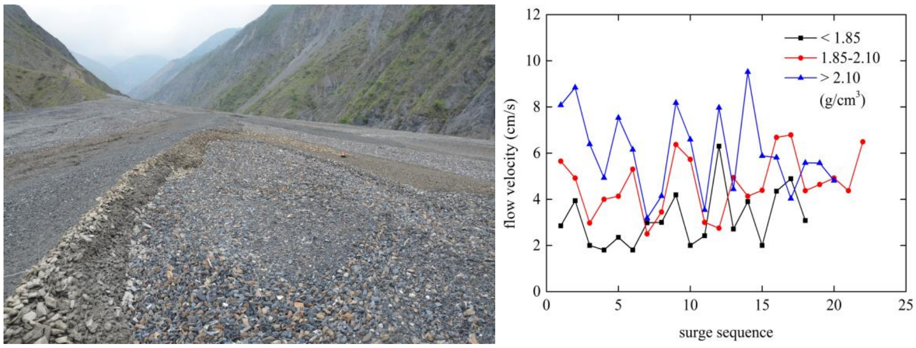


**Fig. 2** Debris flow surges deposit in the mainstream of JJG.

2.2 Data collection

2.2.1 The tributaries divided in JJG

Digital elevation model with spatial resolution 10 m is used in this study to generate elevation and area information, and 81 tributaries are divided into. The tributaries are divided based on field investigation that debris flow easily occurs. Some tributaries in field are displayed in Fig. 3, obviously, there are significant differences in tributaries characteristics, and the study of such tributaries size is of great significance to the formation and occurrence of debris flows. The tributary area varies between $8.7 \times 10^4 \sim 2.07 \times 10^6$ m$^2$ and cover a total area of $4.62 \times 10^7$ m$^2$, about 95% of the whole gully. The serial number of tributary in subregions is presented in Table 1.

Nat. Hazards Earth Syst. Sci. Discuss., https://doi.org/10.5194/nhess-2019-90
Manuscript under review for journal Nat. Hazards Earth Syst. Sci.
Discussion started: 23 April 2019




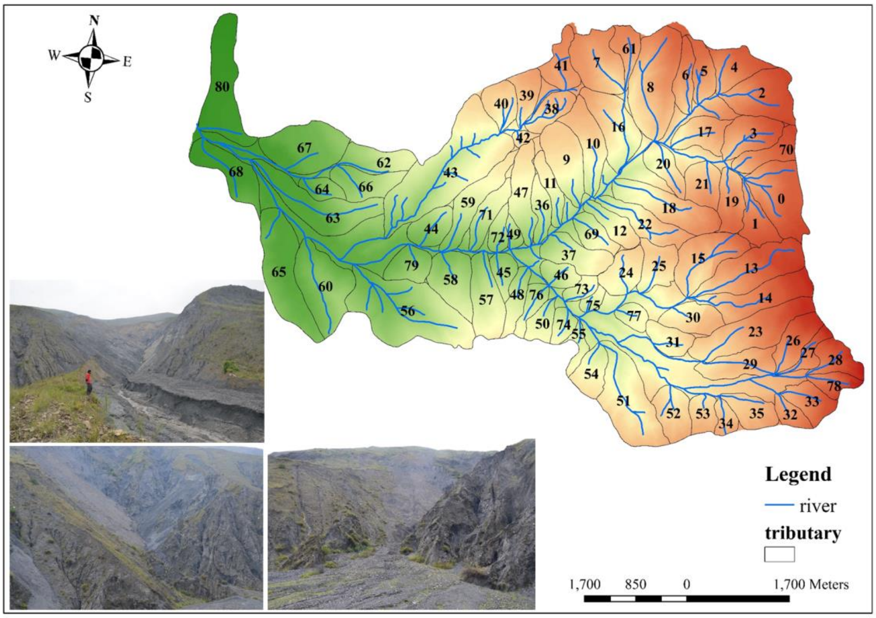


**Fig. 3** The tributaries divided of JJG. Some tributaries in the field are shown on the map.

**Table 1** The tributaries distribution in subregions.

| Subregion | The No. of tributaries |
|---|---|
| Menqian Gully | 2, 4, 5, 6, 7, 8, 9, 10, 11, 12, 16, 17, 18, 20, 22, 36, 37, 47, 49, 61, 69 |
| Duozhao Gully | 13, 14, 15, 23, 24, 25, 26, 27, 28, 31, 31, 32, 33, 34, 35, 45, 46, 48, 50, 51, 52, 53, 54, 55, 73, 74, 75, 76, 77, 78 |
| Upstream | 0, 1, 2, 3, 4, 5, 6, 7, 8, 9, 10, 13, 14, 15, 16, 17, 19, 20, 21, 23, 26, 28, 29, 30, 32, 33, 34, 35, 38, 39, 40, 41, 42, 61, 70 |
| Midstream | 9, 11, 12, 22, 31, 36, 37, 43, 45, 46, 47, 48, 49, 50, 51, 54, 55, 59, 69, 71, 72, 73, 74, 75, 76, 77 |
| Downstream | 44, 56, 58, 60, 62, 63, 64, 65, 66, 67, 68, 79, 80 |

2.2.2 The hypsometric curve and EI

Hypsometric curve for each tributary is calculated. The hypsometric curve is generated by plotting the relative area along the abscissa and the relative height along the ordinate. The relative height can be obtained as the ratio of the height of a given contour (h) from the base plane of the stream mouth to total height of the tributary with reference to the maximum elevation (H), and the relative area is obtained as the ratio of the area above a particular contour (a) to the total area of the tributary encompassing the outlet (A) (Strahler, 1952).

Hypsometric integral is the area between the hypsometric curve (y=h/H and x=a/A) and coordinate axis (Strahler, 1952, 1957), which can be defined as the evolution index (EI).

2.2.3 The extraction of landslides information

Quickbird image of 0.61 m resolution is purchased to create an inventory of landslides. The satellite image is adopted in this study with low cloud shadow coverage, and the aerial coverage of the cloudy area is 0.09 $km^2$ in the study area, about 0.18% of the gully. The atmospheric correction and radiometric correction have been carried out by using the calibration function within the tools of Envi 5.1 software, and 4, 3, 2 bands are combined to false color image stretched of contrast using standard deviation method. Both landslides number and landslides area are necessary to interpret, so the equal area projection is adopted, which has less impact on the landslides area. The landslides information becomes easily extracted on the source image after processing, which is beneficial to the work of visual interpretation, and thus ensures the accuracy of the results.

Landslides are mapped from high resolution satellite data acquired using visual image interpretation on Arc GIS 10.3 software with false color composites or panchromatic images uniformly on 1:5000 scale. The individual landslides initiation zones are indicated using polygons. In the case of complex situations where many landslides are interconnected, it is difficult to identify the individual initiation zones. Use of high resolution images enables demarcation of clustered landslides as individual polygons. The minimum size of landslides area is determined as 0.38 $m^2$ and the area below this value are not considered as the resolution of the satellite image is not sufficient to extract landslides information preferably.

In the interpretation process, we make use of the following diagnostic features: the tone, texture, pattern and shape or form. Meanwhile, direct method, comparison method, integrated reasoning method and other synthetical methods are always used (Dai and Lee, 2002; Kumar et al., 2017; Valenzuela et al., 2017). Using the methods above, 908 landslides have been identified, with area ranging of $3.8 \times 10^{-1} \sim 6.7 \times 10^{5}$ $m^2$. In addition, fieldwork was carried out in May and June 2017. We investigated distribution of 100 landslides with the GPS instrument, and the accuracy achieves 89.21%. The data is used to analyze the relationship between EI with $LA_p$ and LD of each tributary, of which $LA_p$ is landslides area in a tributary/ the tributary area (%) and LD is landslides number in a tributary/ the tributary area (/$10^6$ $m^2$).

Nat. Hazards Earth Syst. Sci. Discuss., https://doi.org/10.5194/nhess-2019-90
Manuscript under review for journal Nat. Hazards Earth Syst. Sci.
Discussion started: 23 April 2019


Natural Hazards and Earth System Sciences
Open Access
Discussions

## 3 Evolution division of JJG

### 3.1 Hypsometric analysis

The hypsometric curves for tributaries are shown in Fig. 4:

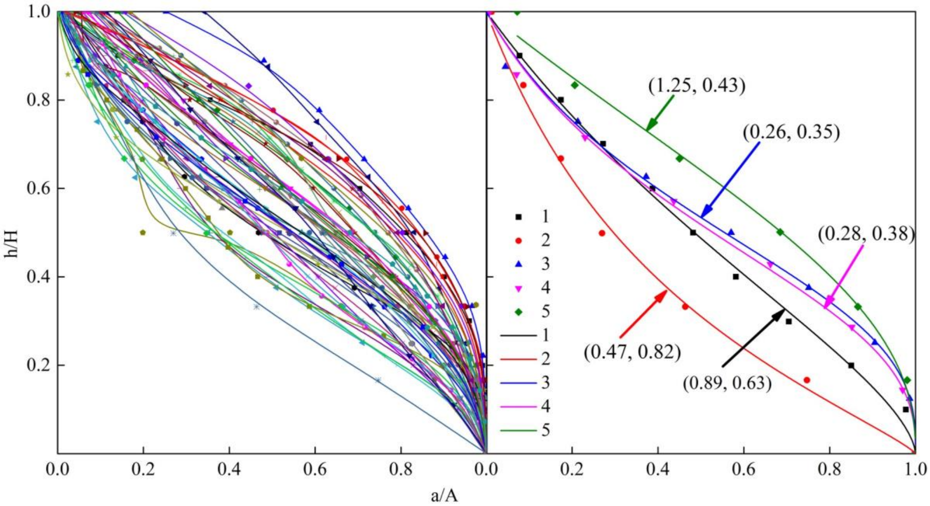


**Fig. 4** The hypsometric curves of different tributaries.

The curves present various types, such as convex, concave and others between them. The curves can be fitted by:

$$y^{1/n} = k(1-x)/(x+k) \qquad (2)$$

Where k and n are parameters. The fitting coefficient $R^2$ achieves 90% above. It is found that higher the curve is, greater the k is. Meanwhile, Fig. 4 shows that with the rising of curves, n is decreasing.

### 3.2 Evolution division of JJG

Then the EI of each tributary in JJG is calculated, which varies from 0.32 to 0.84. According to Strahler, there are three stages: inequilibrium or youthful stage (EI > 0.6), equilibrium or mature stage (EI between 0.3 and 0.6), and monadnock or old stage (EI < 0.3) (Strahler 1952). In order to distinguish the evolution differences of the tributaries, we conduct a more detailed classification and the EI of tributaries in JJG are divided into five groups (Fig. 5):

I (< 0.45), appears in downstream areas and near the outlet of the gully;

II (0.45-0.55), occurs mostly in the Duozhao Gully;

III (0.55-0.65), mostly distributes in midstream and downstream;

IV (0.65-0.75), mostly in midstream and upstream;

V (>0.75), mainly distributes in the headwaters of the Menqian Gully;

Nat. Hazards Earth Syst. Sci. Discuss., https://doi.org/10.5194/nhess-2019-90
Manuscript under review for journal Nat. Hazards Earth Syst. Sci.
Discussion started: 23 April 2019


Natural Hazards and Earth System Sciences
Open Access
Discussions

Moreover, it is found that the EI satisfies the Weibull distribution with the scale parameter of 0.58 and the shape parameter of 6.08 (Fig. 6), the small value of scale parameter means that EI is much concentrated and EI of most tributaries in JJG is between 0.5 and 0.6. According to the frequency distribution of EI, the tributaries of JJG is generally in mature and youthful evolution stages, that is the reason why high frequency debris flow occurred in JJG in the past several decades.

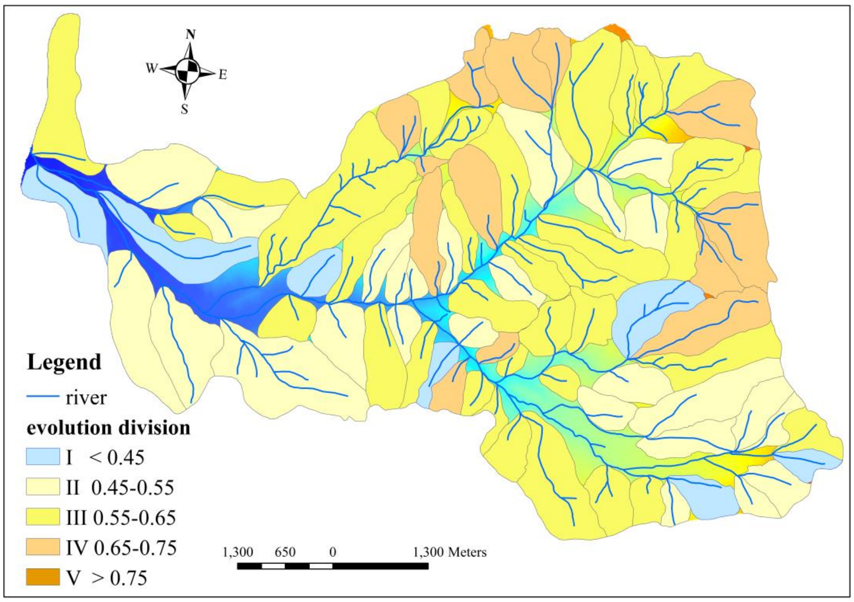


**Fig. 5** The evolution division and EI distribution of tributaries in JJG.

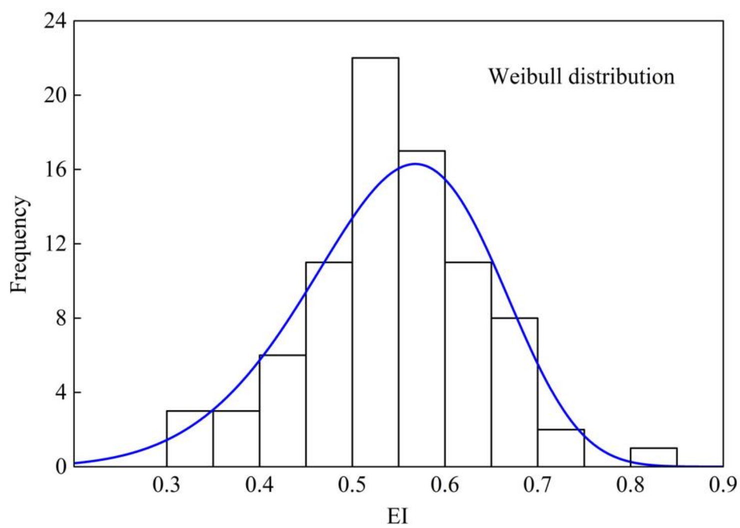

**Fig. 6** The EI frequency distribution of tributaries in JJG.

3.3 Hypsometric curves of different evolution stages

For more clear, we display the hypsometric curves of different evolution stages in Fig.7; in particular, the inflection points of the curves (the rectangle in each plot) are displayed in different position of the curves, they can reflect the geomorphologic features of the tributaries. The inflection point indicates the elevation of a tributary with area varing. When the point is high, the changing occurs at the high elevation, i.e., mainly in the upstream of the tributary.

Obviously, curves in different evolution stages exhibit different characteristics. The bigger the evolution index is, the higher the inflection points of the curves are. In addition, the distribution of inflection points displays distinct spatial features in different evolution stages (Fig. 7).

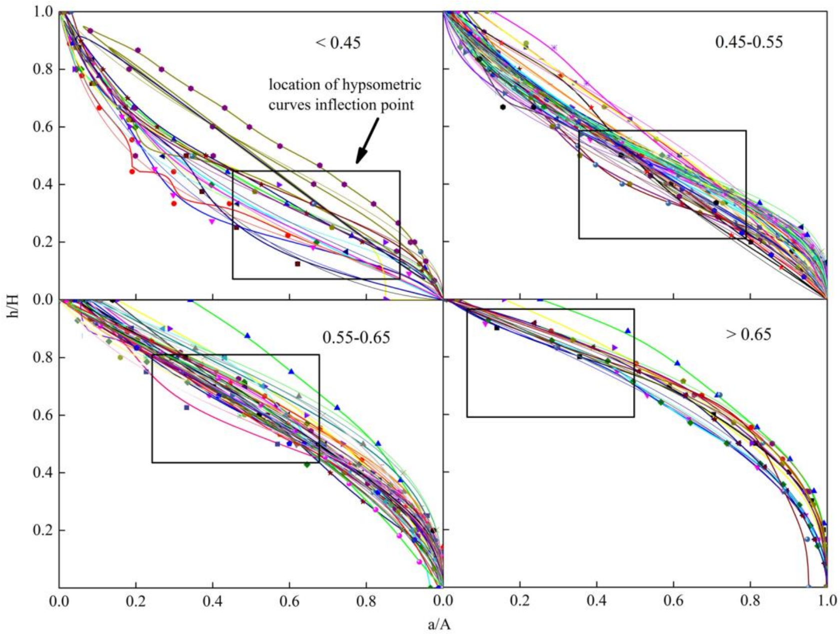


**Fig. 7** Hypsometric curves and the position of inflection points in different evolution stages.

Corresponding to the point h is the area a(h), which is the area in tributary above the inflection point. For a given elevation of point, larger area above it means strong slope process in the upstream. For example, inflection points in EI between 0.45~0.55 are generally higher than those in EI below 0.45, indicating that such tributaries are more prone to landslides activities. Correspondingly, the lower the hypsometric curve is, the more concave the curve is presented, and the smaller of the elevation value corresponding to the inflexion point is, which indicates that the elevation changing in unit area is

Nat. Hazards Earth Syst. Sci. Discuss., https://doi.org/10.5194/nhess-2019-90
Manuscript under review for journal Nat. Hazards Earth Syst. Sci.
Discussion started: 23 April 2019



small, such a tributary is not conducive to the occurrence of landslides.

## 4 Landslides distribution in relation to EI

### 4.1 Landslides distribution of JJG

A total of 908 landslides have been identified, with area ranging from $3.8 \times 10^{-1}$ m$^2$ to $6.7 \times 10^5$ m$^2$. The spatial distribution of landslides is shown in Fig. 8.

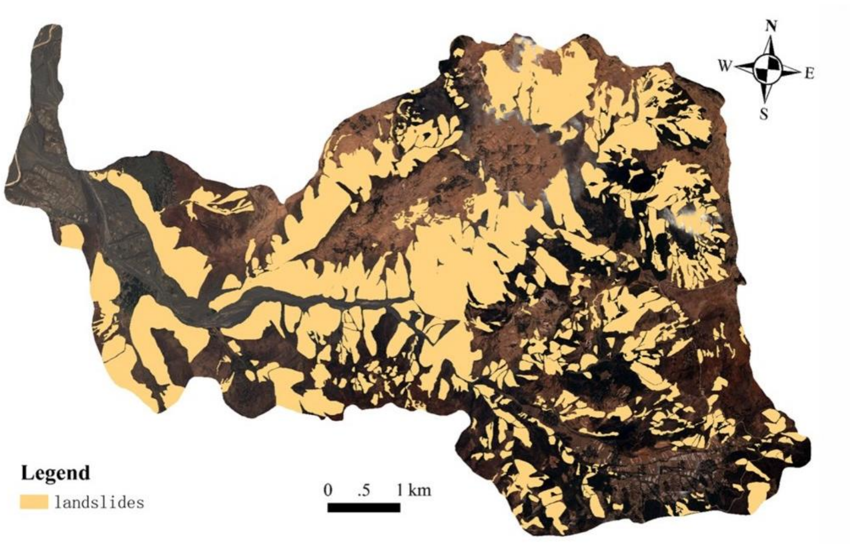


**Fig. 8** Spatial distribution of landslides in JJG.

Landslides are mainly distributed in both sides along the mainstream channels. In details, landslides in Menqian Gully are more concentrated while in Duozhao they are scattering, which is consistent with field observations that landslides are always more frequent in clusters in vulnerable areas.

The landslides distribution in subregions is shown in Table 2, which indicates that $LA_p$ of Menqian Gully is greater than Duozhao Gully, while LD presents a reverse tendency, which means that landslides are concentrated and larger-scale in Menqian Gully, while small landslides are scattering in Duozhao, as seen in Fig. 8. In addition, the $LA_p$ of midstream is greater than upstream and downstream, and LD in upstream is the biggest.

**Table 2** The landslides distribution in subregions.

| Subregion | The area (km$^2$) | The area percentage (%) | Landslides | | | |
|---|---|---|---|---|---|---|
| | | | LA (km$^2$) | $LA_p$ (%) | LN | LD (km$^{-2}$) |

| | | | | | | |
|---|---|---|---|---|---|---|
| Menqian Gully | 12.52 | 27.12 | 5.67 | 45.32 | 248 | 19.81 |
| Duozhao Gully | 15.01 | 32.52 | 4.62 | 30.81 | 403 | 26.85 |
| Upstream | 19.60 | 42.47 | 6.22 | 31.71 | 526 | 26.83 |
| Midstream | 16.46 | 35.66 | 7.55 | 45.88 | 356 | 21.63 |
| Downstream | 10.71 | 23.21 | 3.50 | 32.71 | 67 | 6.25 |

4.2 Landslides distribution in different evolution division

4.2.1 The landslides distribution related to evolution stages of all tributaries

The evolution division and landslides distribution layers are overlaid to form the spatial distribution map, as shown in Fig. 9. It is clear that major of landslides are distributed in subregions of III and IV, with EI between 0.55 ~ 0.75.

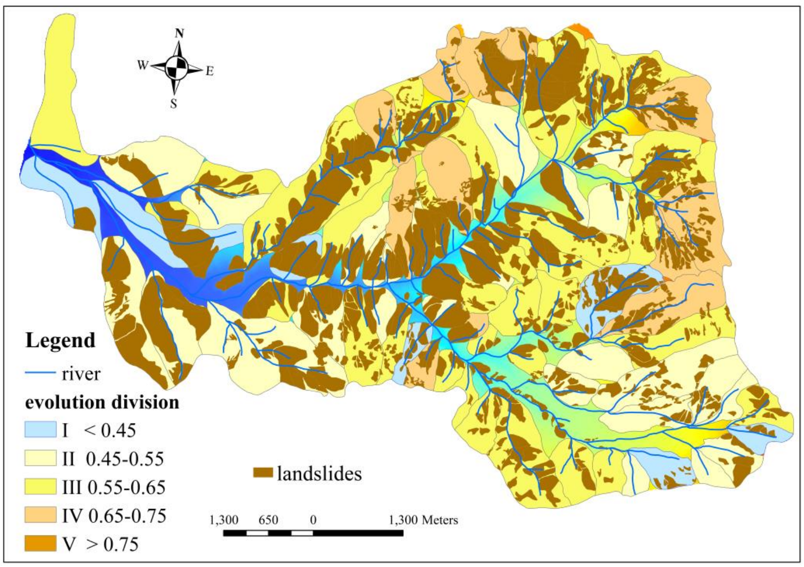


**Fig. 9** Landslides distribution in various evolution stages.

Fig. 10 shows how LD and $LA_p$ vary with EI. It shows that LD increases exponentially with EI increasing, which means that more landslides occur in the tributaries at younger evolutionary stage. Meanwhile, the greater fluctuation of $LA_p$ is in tributaries with the range of EI less than 0.54, while a smaller fluctuation is in tributaries of EI more than 0.54, and the $LA_p$ is generally smaller than other evolution stages in active evolution stage.

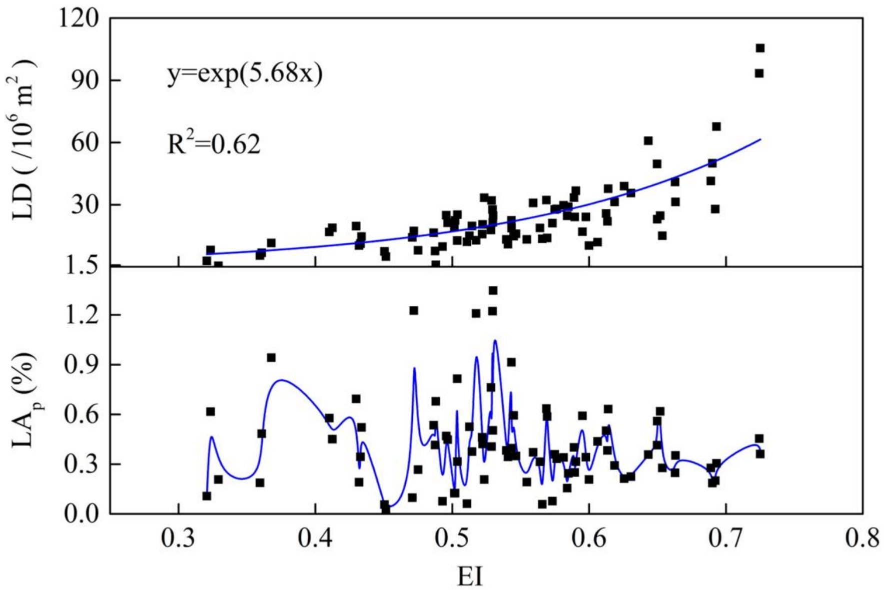


**Fig. 10** Relationship between landslides and EI.

The percentage of $LA_p$ increases at the range of less than 0.52 and decreases at the range of more than 0.52 approximatively. The $LA_p$ is generally greater in the range of EI smaller than 0.55, and $LA_p$ decreases clearly with EI exceeding 0.52. Therefore, more landslides mainly occur in active stages on small scale.

4.2.2 Landslides distribution in typical subregions

The major branches of JJG, the Gully of Menqian and Duozhao, are distinctive in debris flow and landslides activities. As mentioned above, landslides are more scattering in Duozhao and more concentrated in Menqian. Now we consider how landslides distribute in tributaries in these subregions.

Fig. 11 shows that in both gullies LD increases exponentially with EI, almost in the same exponential function. As for $LA_p$, several peaks occur in different EI values in Menqian Gully but only a single peak occurs (around EI with 0.55) in Duozhao Gully, meaning that landslides are widely distributed in tributaries with EI >0.45 in Menqian Gully.

Nat. Hazards Earth Syst. Sci. Discuss., https://doi.org/10.5194/nhess-2019-90
Manuscript under review for journal Nat. Hazards Earth Syst. Sci.
Discussion started: 23 April 2019


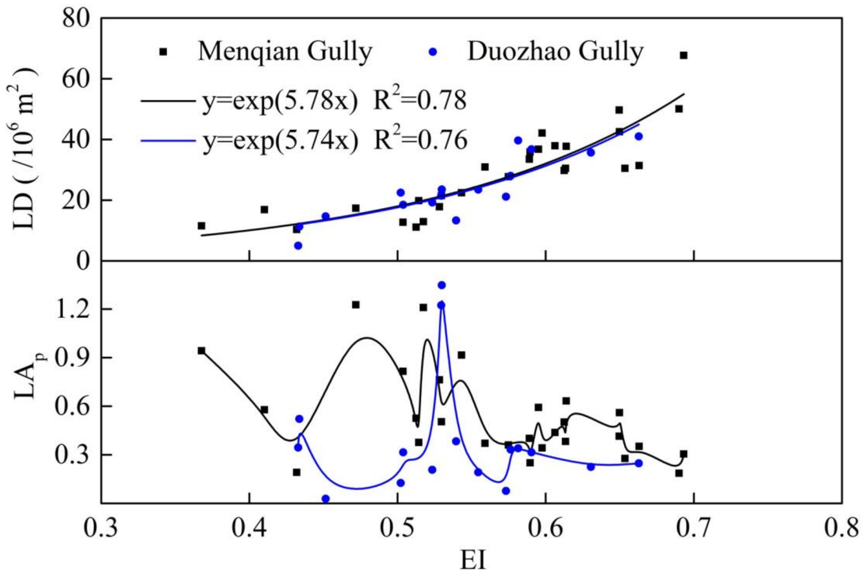


**Fig. 11** Relationship between landslides and EI in typical gullies.

Similarly, we consider LD and $LA_p$ in the regions of the upstream, midstream and downstream in JJG that have visible terrain difference, as shown in Fig. 12. Again it is found that LD increases exponentially with EI both in the upstream and midstream.

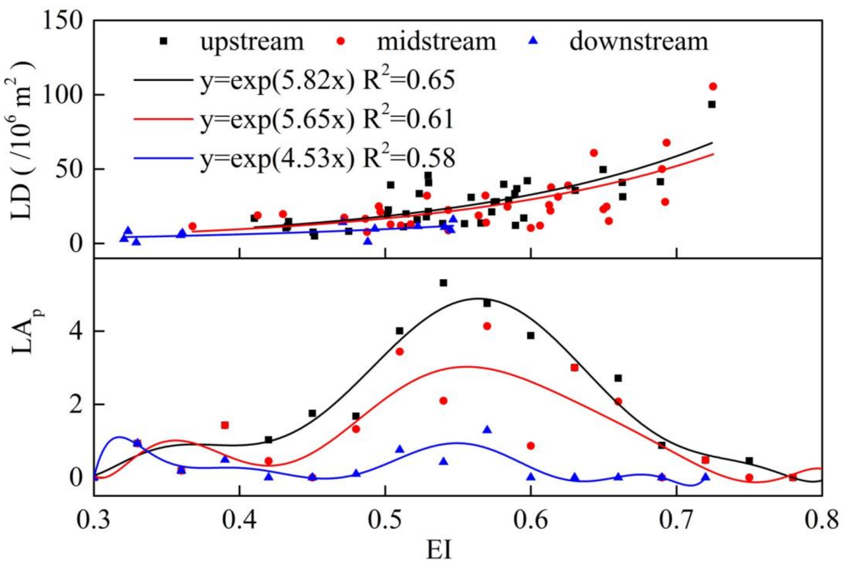


**Fig. 12** Relationship between landslides and EI in subregions.

$LA_p$ mainly increases first and then decreases as EI increases, and the $LA_p$-EI curve in the range of less than 0.54 is higher than the range of more than 0.54, which has the similar tendency with the $LA_p$-EI curve in all tributaries of JJG. Also the $LA_p$ in upstream and midstream is higher than upstream, lower $LA_p$ exists in tributaries at the younger evolutionary stages. Meanwhile, lower LD and larger $LA_p$ is in the downstream, which is at the old evolution stage, which means that with the occurrence of historical landslides or large landslides in slope surface, the tributary has reached a stable state.

## 5 Discussion

### 5.1 The Power-law frequency verification of landslides distribution

Power-law frequency-magnitude relationship has been generally observed for landslides at a wide range of size (Hovius et al., 1997; Stark and Hovius, 2001; Malamud et al., 2010), but for a small-scale gully like JJG there is no report in literatures. For the landslides in JJG, the power law is perfectly valid (Fig. 13), with exponent being 4.32, which differs much from the exponent for landslides over large scale regions, such as those in the Gorkha area (2.5), the Northridge, California (2.30), and the Wenchuan area (2.19), and many other regions (Eeckhaut et al., 2007; Lari et al., 2014). The verification of power law confirms that the landslides area interpreted is reliable.

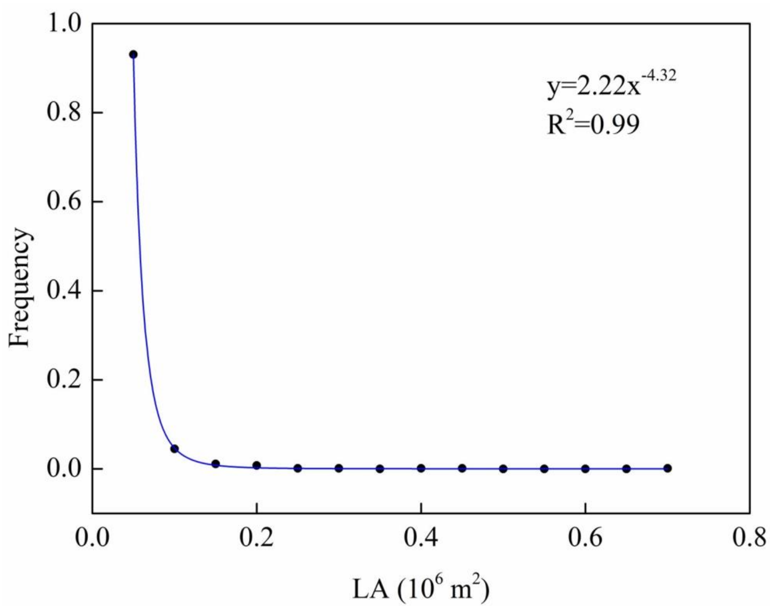


**Fig. 13** The landslide area frequency distribution of JJG.

Meanwhile, both LD and $LA_p$ are found to satisfy the Weibull distribution, with the shape parameter and scale parameter being 1.44 and 26.86 for LD and 1.62 and 0.64 for $LA_p$, respectively (Fig. 14). The higher scale parameter of LD suggests that LD is more sensitive to tributary distinction.

Nat. Hazards Earth Syst. Sci. Discuss., https://doi.org/10.5194/nhess-2019-90
Manuscript under review for journal Nat. Hazards Earth Syst. Sci.
Discussion started: 23 April 2019

Natural Hazards and Earth System Sciences
Open Access
Discussions

Meanwhile, the peak of frequency curve of LD is 11.86 and 0.22 of $LA_p$, which indicates that the landslides of most tributaries are distributed on small scales.

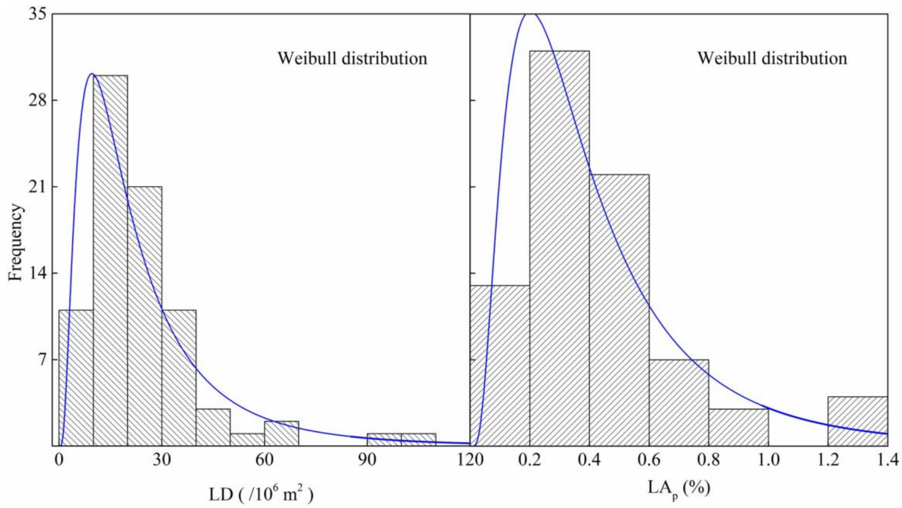


**Fig. 14** The frequency distribution of landslides among tributaries.

5.2 Distribution of EI

In JJG, EI of tributaries satisfies the Weibull distribution with scale and shape parameter of 0.58 and 6.08, this is comparable to the EI distribution of tributaries in the Wenchuan earthquake region where the scale and shape parameter is 0.53 and 11.73, respectively (Fig. 15). The scale parameter can reflect the EI range of variation, which varies between 0.38 and 0.64 in the Wenchuan area and betweem 0.32 and 0.84 in JJG. The difference here can be attributed that a number of tributaries in JJG having no landslides, while in Wenchuan, landslides distribute in almost every tributary. This also implies that landslides occur in tributaries within a relatively narrow range of EI. More important point is the difference between shape parameters, the bigger shape parameter in Wenchuan region means that the curve is to the right more than in JJG, implying that the earthquake is inclined to induce more landslides in tributaries of big EI. As JJG is of tributaries with wide range evolution stages, we choose it as the study area to reveal the mechanism of landslides distribution.

Nat. Hazards Earth Syst. Sci. Discuss., https://doi.org/10.5194/nhess-2019-90
Manuscript under review for journal Nat. Hazards Earth Syst. Sci.
Discussion started: 23 April 2019

Natural Hazards and Earth System Sciences Discussions

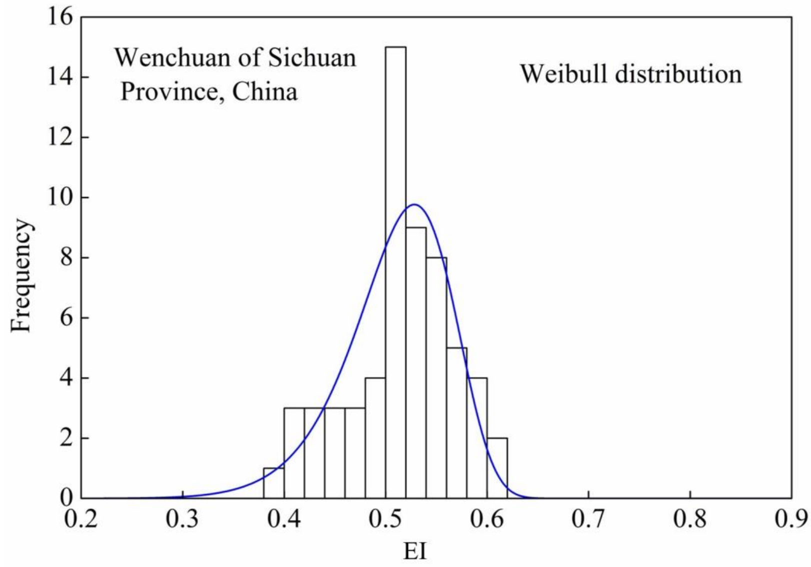


**Fig. 15** The EI frequency distribution of Wenchuan in Sichuan province.

5.3 EI and tributary morphological features

5.3.1 EI and slope distribution

As a comprehensive topography index, EI reflects the geomorphology characteristics of the tributary. Fig. 16 shows how slope varies with EI on average, as it is crucial for landslides and debris flow formation. The maximal average slope, usually bigger than the friction angle of the soil, occur mainly between EI of 0.5-0.65, this coincides with range of most landslides distribution, and this also accounts for the relationship between EI and LD which indicates that EI is related to the number or frequency of landslides. Meanwhile, the landslides are concentrated in tributaries of class III (EI = 0.55~0.65), and these tributaries are concentrated in the midstream and upstream, mainly in the Menqian Gully. The landslides distribution in tributaries of different EI quantitatively reveals spatial heterogeneity distribution. The spatial distinction of landslides distribution results from the diverse evolution stages of tributaries, which provides a heterogeneous background for material supplying in gully. The spatial heterogeneity distribution can reveal the reason why landslides are frequent in some tributaries while occasional in others, thus roughly to predict the landslides activity of tributaries, which is of great significance to the comprehensive management of small watershed.

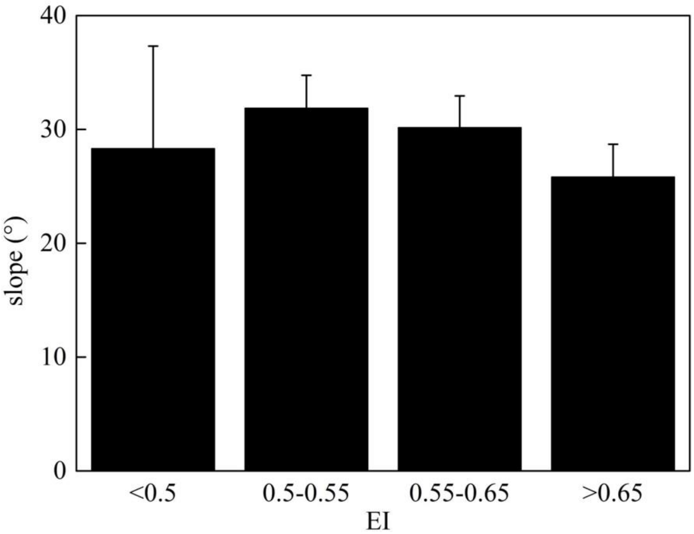


**Fig. 16** Slope variation in different evolution stages.

5.3.2 EI and channel density

Debris flow converging from tributaries into mainstream channel depends on the flow routes, or the stream length of each tributary, and this can be described by the channel density (i.e., the length in unit area of a region). Fig. 17 shows the density variation with EI, indicating that the channel density of tributary is increasing as EI rises, which is conducive to the occurrence of debris flow activity.

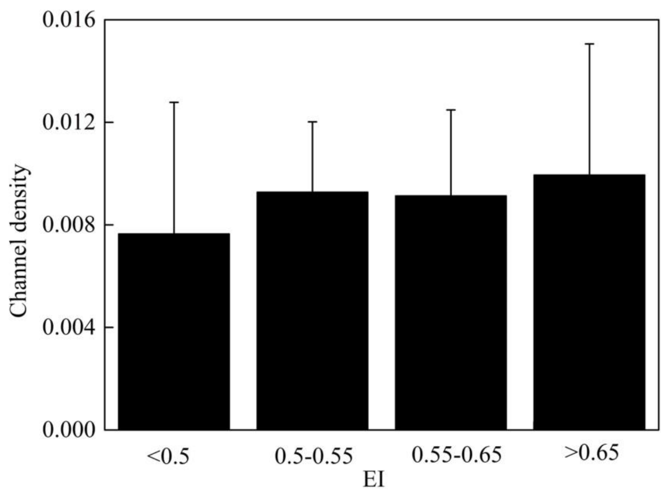


**Fig. 17** Channel density variation in different evolution stages.

Then the tributaries of EI between 0.5 and 0.65 provide favorable condition both for landslides and flow convergence, and thus facilitate the forming and developing of debris flows.

5.4 Implication in debris flow surges

The spatial heterogeneity of tributary distribution reveals the variety of debris flow sources. As it is difficult to observe the debris flows of each tributary, we usually see the convergence debris flows from multiple sources. Debris flow surges always present the characteristic of diverse forms from the perspective of material supplies (Li et al., 2015), and this can be attributed to the spatial heterogeneity of evolution and landslides activity of tributaries as discussed above.

Previous studies usually consider debris flows activity on the gully scale and ignore the distinction on tributary scale (Chen and Wang, 2017; Malet et al., 2004), they cannot tell the feature of debris flows from multiple sources and undergoing diverse tributaries processes, such as initiation on slope, flow downwards in tributary channel, and confluence into the mainstream, all closely related to the tributary feature.

Besides, the formation of debris flow is activated by rainfall (Chen et al., 2006; Fuchu et al., 1999; Fusco et al., 2017; Kuo and Chuan, 2007; McArdell et al., 2007; Reneau and Dietrich, 1987; Tan and Han, 1992), different rainfall intensity and amount is in different tributaries, which adds more diversity to the surges. The factor of precipitation will be the next study to consider and understand the formation mechanism of debris flow surges.

## 6 Conclusions

This study has revealed the spatial heterogeneity of a debris flow gully through landslides distribution in tributaries of different evolution stages. It is found that most landslides are distributed in the relative young tributaries (with evolution index between 0.5 ~ 0.6). Generally, the LD increases exponentially with EI and the $LA_p$ is concentrated in EI between 0.5 and 0.6, in accordance with the general landslides distribution. Meanwhile, the EI satisfies the Weibull distribution, such distribution feature also occurs in the Wenchuan area.

The majority of tributaries are at the EI range between 0.5 and 0.6, which means that sufficient material from landslides for debris flows can be provided, which explains the reason that JJG has the debris flow a of high frequency. In addition, the landslides distribution in JJG reveals the nonuniform distribution of material sources for debris flows, which provides the fundamental evidence for the variety of debris flow surges.

**Acknowledgments**

This research is supported by the National Natural Science Foundation of China (grant no. 41471011), Key International S&T Cooperation Academy of Sciences (grant no. 2016YFE0122400).

**References**

Arai, M.: A research on unsteady period of debris flow surges. EGU General Assembly Conference Abstracts 19, 10715, 2017.

Bartolini, C., D'Agostino, N., and Dramis, F.: Topography, exhumation, and drainage network evolution of the apennines. Episodes 26, 212-216, 2003.

Baum, R. L., Coe, J. A., Godt, J. W., Harp, E. L., Reid, M. E., Savage, W. Z., Schulz, W. H., Brien, D. L., Chleborad, A. F., and McKenna, J. P.: Regional landslide-hazard assessment for seattle, washington, USA. Landslides 2, 266-279, 2005.

Beguería, S.: Changes in land cover and shallow landslide activity: A case study in the spanish pyrenees. Geomorphology 74, 196-206, 2006.

Berger, C., McArdell, B. W., and Schlunegger, F.: Sediment transfer patterns at the illgraben catchment, switzerland: Implications for the time scales of debris flow activities. Geomorphology 125, 421-432, 2011.

Blahut, J., Westen, C. J. V., and Sterlacchini, S.: Analysis of landslide inventories for accurate prediction of debris-flow source areas. Geomorphology 119, 36-51, 2010.

Bollschweiler, M., Stoffel, M., Ehmisch, M., and Monbaron, M.: Reconstructing spatio-temporal patterns of debris-flow activity using dendrogeomorphological methods. Geomorphology 87, 337-351, 2007.

Chen, C. Y., and Wang, Q.: Debris flow-induced topographic changes: Effects of recurrent debris flow initiation. Environmental monitoring and assessment 189, 449, 2017.

Chen, H., Dadson, S., and Chi, Y. G.: Recent rainfall-induced landslides and debris flow in northern taiwan. Geomorphology 77, 112-125, 2006.

Dai, F., and Lee, C.: Landslide characteristics and slope instability modeling using gis, lantau island, hong kong. Geomorphology 42, 213-228, 2002.

Eeckhaut, M. V. D., Poesen, J., Govers, G., Verstraeten, G., and Demoulin, A.: Characteristics of the size distribution of recent and historical landslides in a populated hilly region. Earth & Planetary

Nat. Hazards Earth Syst. Sci. Discuss., https://doi.org/10.5194/nhess-2019-90
Manuscript under review for journal Nat. Hazards Earth Syst. Sci.
Discussion started: 23 April 2019


Science Letters 256, 588-603, 2007.

Fuchu, D., Lee, C., and Sijing, W.: Analysis of rainstorm-induced slide-debris flows on natural terrain of lantau island, hong kong. Engineering Geology 51, 279-290, 1999.

Fusco, F., Allocca, V., and Vita, P. D.: Hydro-geomorphological modelling of ash-fall pyroclastic soils for debris flow initiation and groundwater recharge in campania (southern italy). Catena 158, 235-249, 2017.

Gabet, E. J., and Mudd, S. M.: The mobilization of debris flows from shallow landslides. Geomorphology 74, 207-218, 2006.

Hamza, V., Prasannakumar, V., and Pratheesh, P.: Landform evaluation through hypsometric characterisation: an example from selected river basin in southern western ghats, india 73, 4, 2018.

Hovius, N., Stark, C. P., and Allen, P. A.: Sediment flux from a mountain belt derived from landslide mapping. Geology 25, 231-234, 1997.

Huggel, C., Clague, J. J., and Korup, O.: Is climate change responsible for changing landslide activity in high mountains? Earth Surface Processes and Landforms 37, 77-91, 2012.

Kumar, D., Thakur, M., Dubey, C. S., and Shukla, D. P.: Landslide Susceptibility Mapping & Prediction using Support Vector Machine for Mandakini River Basin, Garhwal Himalaya, India. Geomorphology 295, 2017.

Kuo, L., and Chuan, T.: Progress in research on debris flow hazard assessment. Journal of Catastrophology 1, 023, 2007.

Langebein, W. B., and Basil, W.: Topographic characteristics of drainage basins. USGS Water Supply Paper 947-C, 1947.

Lari, S., Frattini, P., and Crosta, G. B.: A probabilistic approach for landslide hazard analysis. Engineering Geology 182, 3-14, 2014.

Li, Y., Su, P. C., and Su, F. H.: Debris flow as a spatial poisson process. Journal of Mountain Science 29, 586-590, 2011 (In Chinese).

Li, Y., Liu, J. J., Hu, K. H., and Su, P. C.: Probability distribution of measured debris-flow velocity in jiangjia gully, yunnan province, china. Natural hazards 60, 689-701, 2012.

Li, Y., Zhou, X. J., Su, P. C., Kong, Y. D., and Liu, J. J.: A scaling distribution for grain composition of debris flow. Geomorphology 192, 30-42, 2013.

Nat. Hazards Earth Syst. Sci. Discuss., https://doi.org/10.5194/nhess-2019-90
Manuscript under review for journal Nat. Hazards Earth Syst. Sci.
Discussion started: 23 April 2019




Li, Y., Liu, J. J., Su, F. H., Xie, J., and Wang, B. L.: Relationship between grain composition and debris flow characteristics: A case study of the jiangjia gully in china. Landslides 12, 19-28, 2015.

Lv, X. J., Liu, X. L., and Su, P. C.: The Area-altitude Analysis on the Evolution Stage of Debris Flow Ravines :Taking Daqu River as an Example. Journal of Mountain Science 23, 336-341, 2005 (In Chinese).

Malet, J. P., Maquaire, O., Locat, J., and Remaître, A.: Assessing debris flow hazards associated with slow moving landslides: methodology and numerical analyses. Landslides 1, 83-90, 2004.

Martha, T. R., Roy, P., Mazumdar, R., Govindharaj, K. B., and Kumar, K. V.: Spatial characteristics of landslides triggered by the 2015 m w, 7.8 (gorkha) and m w, 7.3 (dolakha) earthquakes in nepal. Landslides 1-8, 2016.

McArdell, B. W., Bartelt, P., and Kowalski, J.: Field observations of basal forces and fluid pore pressure in a debris flow. Geophysical Research Letters 34, 248-265, 2007.

Malamud, B. D., Turcotte, D. L., Guzzetti, F., and Reichenbach, P.: Landslide inventories and their statistical properties, Earth Surface Processes & Landforms 29, 687-711, 2010.

Pike, R. J., and Wilson, S. E.: Elevation-relief ratio, hypsometric integral, and geomorphic area-altitude analysis. Geological Society of America Bulletin 82, 1079-1084, 1971.

Pradhan, B., and Sameen, M. I.: Landslide susceptibility modeling: Optimization and factor effect analysis. Laser scanning applications in landslide assessment, Springer 115-132, 2017.

Reneau, S. L., and Dietrich, W. E.: The importance of hollows in debris flow studies; examples from marin county, california. Reviews in engineering geology 7, 165-180, 1987.

Schumm, S. A.: Evolution of drainage systems and slopes in badlands at Perth Amboy, New Jersey[J]. Bulletin of the Geological Society of America 67, 597-646, 1956.

Strahler, A.: Hypsomic analysis of erosional topography. Bulletin of Geol. Soc. of America 63, 1117–1142, 1952.

Stark, C. P., and Hovius, N.: The characterization of landslide size distributions. Geophysical Research Letters 28, 1091-1094, 2001.

Strahler, A. N.: Quantitative analysis of watershed geomorphology. Eos, Transactions American Geophysical Union 38, 913-920, 1957.

Tan, W. P., and Han, Q. Y.: Study on regional critical rainfall indices of debris flow in Sichuan province. Journal of catastrophology 7, 37-42, 1992.

Nat. Hazards Earth Syst. Sci. Discuss., https://doi.org/10.5194/nhess-2019-90
Manuscript under review for journal Nat. Hazards Earth Syst. Sci.
Discussion started: 23 April 2019


Natural Hazards and Earth System Sciences
Open Access
Discussions

Valenzuela, P., Domínguez-Cuesta, M. J., García, M. A. M., and Jiménez-Sánchez, M.: A spatio-temporal landslide inventory for the NW of Spain: BAPA database. Geomorphology 293, 11-23, 2017.

Wang, C., Esaki, T., Xie, M., and Qiu, C.: Landslide and debris-flow hazard analysis and prediction using gis in minamata–hougawachi area, japan. Environmental Geology 51, 91-102, 2006.

Webb, R. H., Pringle, P. T., and Rink, G. R.: Debris flows from tributaries of the colorado river, grand canyon national park, arizona. United States Geological Survey, Professional Paper 1492, 1989.

Wieczorek, G. F.: Landslide triggering mechanisms. Landslides: Investigation and mitigation 247, 76-90, 1996.

Wieczorek, G. F., and Glade, T.: Climatic factors influencing occurrence of debris flows. Debris-flow Hazards and Related Phenomena. Springer Berlin Heidelberg, pp. 325-362, 2005.

Wu, J., Kang, Z., Tian, L., and Zhang, S.: Observation and research of debris flow in Jiangjiagou Ravine, Yunnan Province. Science Pressing, Beijing, pp. 67–145, 1990.

Xiang, L. Z., Li, Y., Chen, H. K., Su, F. H., and Huang, X.: Sensitivity analysis of debris flows based on basin evolution. Resources and environment of the Yangtze river basin 24, 1984-1992, 2015 (In Chinese).

Zhuang J. Q., Cui, P., Wang, G. H., Chen, X. Q., and Guo, X. J.: Rainfall thresholds for the occurrence of debris flows in the Jiangjia Gully, Yunnan Province, China. Engineering Geology 195, 335-346, 2015.